Available on CMS information server

CMS CR -2009/189

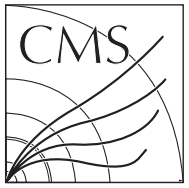

The Compact Muon Solenoid Experiment

Conference Report

Mailing address: CMS CERN, CH-1211 GENEVA 23, Switzerland

15 July 2009 (v3, 19 July 2009)

QCD Physics Potential of CMS

K. Rabbertz on behalf of the CMS Collaboration

Abstract

In view of the approaching LHC operation the feasibility and accuracy of QCD measurements with the CMS experiment at the Large Hadron Collider (LHC) involving hadrons and jets are discussed. This summary is based on analyses performed at CMS for center-of-mass energies of 10 as well as $14\,\mathrm{TeV}$ assuming event numbers ranging from some days of data taking up to $10\,\mathrm{pb}^{-1}$ of integrated luminosity with proton-proton collisions.

Presented at *1st IPM Meeting on LHC Physics,20.-24. April 2009,Isfahan,Iran,01/08/2009*

1 Introduction

With the advent of the LHC, a completely new regime in centre-of-mass energy for hadron-hadron collisions will be explored. While the main interest of the LHC is to unravel the nature of electroweak symmetry breaking, a detailed understanding of the detector performance and the Standard Model processes is a must. QCD, the theory of the strong interaction, describes one of the four fundamental forces of nature and in particular the hard interactions between coloured quarks and gluons and how they bind together to form hadrons. Due to the huge cross sections of QCD reactions involved, the most outstanding feature of events at the TeV energy scale is therefore the abundant production of jets, i.e. collimated streams of hadrons that are supposed to originate from a common initiator. A profound understanding of hadron production and jet physics therefore poses the foundation for the physics commissioning and monitoring of the CMS experiment [1] and is a mandatory step in order to re-establish the Standard Model and to set the stage for the search of new phenomena.

In the next section analyses dealing with first measurements of hadron production and of the Underlying Event (UE) activity based on jets formed from tracks of charged particles are presented. The following section then concentrates on jet physics before finishing this report with an outlook.

Photon physics which in CMS is included in the QCD working group as well had to be left out. The latest results from CMS can be found in [2] and [3]. Details on the performance of the CMS experiment with respect to track reconstruction, alignment, jet finding and calibration can be found elsewhere in these proceedings.

2 Tracks and Hadrons

2.1 Charged Hadron Production

Charged particle multiplicity distributions from hadron-hadron collisions have been studied already in other experiments [4, 5]. A measurement of the distribution in pseudorapidity $\eta = -\ln\tan(\theta/2)$ with θ being the polar angle, $dN_{ch}/d\eta$, can be carried out with a few thousand events collected by the CMS detector and will be one of the first measurements at the LHC. Since one has to integrate over the transverse momentum spectrum for each pseudorapidity region, however, one needs to extrapolate the measurable p_{T} range to small momenta due to the limitation of track finding in the low p_{T} limit. To reduce unavoidable modeling systematics three different methods to reach as low in p_{T} as possible are foreseen in CMS [6–8].

The first consists of a hit-counting technique [9] where charged particles are only required to reach the first layer of the CMS pixel detector, hence $p_{\mathrm{T}} \gtrsim 30\,\mathrm{MeV}$. The advantage of this method is its relative insensitivity to detector misalignment, however, it depends on details of the simulation of the pixel response. The results from all three pixel layers (with different reaches in low p_{T}) can be compared. To reduce the sensitivity to the detailed detector response simulation, tracklets consisting of two-hit pixel tracks in consecutive layers are employed as suggested in [10]. Finally, a track-reconstruction method with pixel hit triplets working down to $p_{\mathrm{T}} \approx 100\,\mathrm{MeV}$ is proposed which requires a more careful study of the tracker alignment. The three techniques exhibit different sensitivities to the diverse sources of systematic uncertainty and complement each other. Simulation results for all three are shown in figure 1.

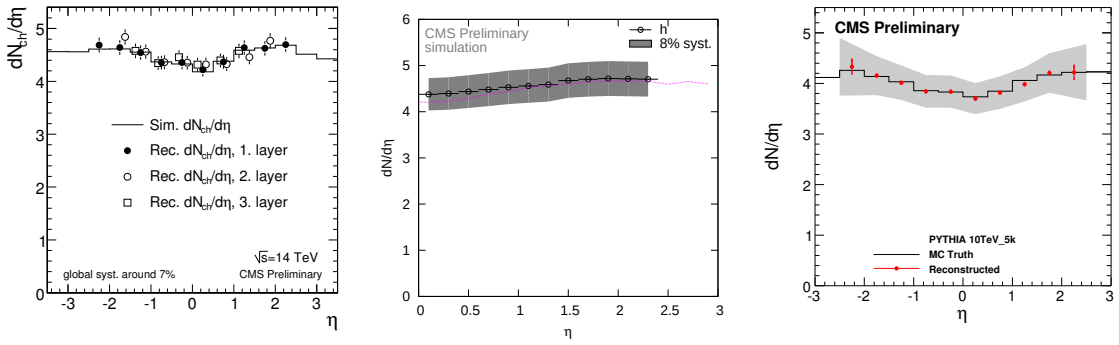

Figure 1: Simulation results for charged particle densities in pseudorapidity using the methods of pixel hit counting (left, $\sqrt{s} = 14\,\mathrm{TeV}$), pixel tracklets (middle, $\sqrt{s} = 10\,\mathrm{TeV}$) and track reconstruction with pixel triplets (right, $\sqrt{s} = 10\,\mathrm{TeV}$) including estimates of the systematic uncertainties of $\approx 7 - 10\%$ are shown together with input predictions from PYTHIA.

2.2 Underlying Event Measurements

Another analysis [11] exploits the standard track reconstruction for $p_{\mathrm{T}} > 900\,\mathrm{MeV}$ with the silicon strip tracker of CMS. After triggering on Minimum Bias or jet events with different jet p_{T} thresholds, all the tracks are investigated with respect to the difference in azimuth towards the leading jet constructed from these tracks. In other experiments [12, 13] it could be shown that the transverse region of $60° < |\Delta\phi| < 120°$ with respect to the leading jet is most sensitive to the Underlying Event, i.e. every collision product not coming directly from the hard scatter. Extrapolations of the UE contributions to events at LHC energies vary widely such that an early determination of its size and the tuning of the MC generators is an important start-up measurement.

Figure 2 presents the composition of the total charged particle distribution in $\Delta\phi$ for all trigger streams on the left and the resulting p_{T} dependence of the charged particle density in the transverse plane reconstructed from simulations with PYTHIA tune DWT on the right. For comparison the MC predictions of PYTHIA with various tunes and from HERWIG without model for multiple parton interactions are shown as well. Already with the assumed $10\,\mathrm{pb}^{-1}$ of integrated luminosity at $\sqrt{s} = 14\,\mathrm{TeV}$ it will be possible to differentiate between the extrapolations of some models to LHC energies. Using tracks with a lower limit of $p_{\mathrm{T}} > 500\,\mathrm{MeV}$ the sensitivity can be further increased as demonstrated in [11].

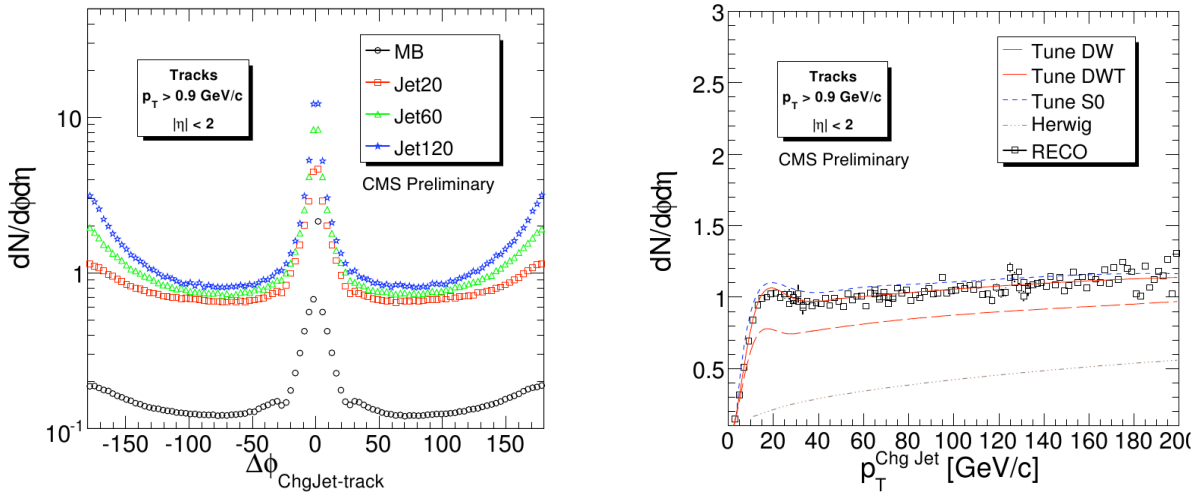

Figure 2: Composition of the total charged particle distribution in $\Delta\phi$ for all trigger streams (left) and the resulting p_{T} dependence of the reconstructed charged particle density in the transverse plane together with predictions of various PYTHIA tunes and from HERWIG assuming $10\,\mathrm{pb}^{-1}$ of integrated luminosity at $\sqrt{s} = 14\,\mathrm{TeV}$.

3 Jet Physics

In contrast to the last section where jets were used at most in order to fix the basic orientation of an event, they are the primary topic now. Instead of looking after global event properties like the numbers of produced hadrons or the general flow of momentum in an event, one would like to establish a closer connection to the hard process which is described theoretically in terms of partons, i.e. quarks, anti-quarks and gluons. Since it is impossible to unambiguously assign bunches of observed hadrons to the originating partons, jet algorithms are employed that define a distance measure between objects and uniquely determine which of them are sufficiently close to each other to be considered to come from the same origin and hence to combine them into a jet.

In CMS three jet algorithms with in total five different jet sizes R (or D) are in use: The Iterative Cone algorithm with $R = 0.5$ as implemented in the trigger of the CMS experiment [14], the SISCone algorithm [15] with $R = 0.5$ or $R = 0.7$, and the k_{T} algorithm [16–18] with $D = 0.4$ or $D = 0.6$. For SISCone and k_{T} the implementation of [19] has been employed. It has to be noted that the Iterative Cone is not collinear and infrared-safe.

For safe jet algorithms the following theoretical uncertainties in approximate order of importance have to be considered when comparing pQCD results to experimental data: The uncertainty inherent in the determination of the parton density functions (PDFs) of the proton, the precision in perturbative QCD (leading order LO, next-to-leading order NLO, ...) [1)], non-perturbative corrections, the dependence on the PDF parameterizations, the knowledge of $\alpha_S(M_Z)$, and for very high jet transverse momenta potentially electroweak corrections.

[1)] The uncertainty of a pQCD calculation is conventionally estimated by varying the renormalization and factorization scales.

On the experimental side the dominant uncertainties are due to the jet energy calibration JEC (including the treatment of electronic noise and of collisions from different proton bunch crossings, i.e. pile-up), the luminosity determination, the jet energy resolution JER, trigger efficiencies, the spatial resolutions in azimuthal angle ϕ and in pseudorapidity η, and non-collision background. Depending on a particular jet analysis the sensitivity to one or another effect might be reduced. For example in the case of normalized observables like the dijet azimuthal decorrelation and event shapes or in cross-section ratios like the dijet production ratio in pseudorapidity and 3-jet to all-jet ratios, the luminosity uncertainty is eliminated and the uncertainty due to the JEC is reduced. The inclusive jet cross section, which will be discussed first, is a particularly challenging measurement and requires all uncertainties to be under control.

3.1 Inclusive Jets

In [20] a plan for the measurement of the differential inclusive jet production cross section for rapidities up to $|y| = 2.5$ with CMS assuming $10\,\mathrm{pb}^{-1}$ of integrated luminosity at a center of mass energy of $\sqrt{s} = 10\,\mathrm{TeV}$ is presented.[2)] The reach in jet transverse momentum is already beyond any previous collider experiment [22–24] and the TeV scale of jet physics can be probed. The analysis is performed on fully simulated CMS events which are adopted as pseudo data. Jets are reconstructed from calorimeter energy depositions with the inclusive k_T ($D = 0.6$) and the SISCone ($R = 0.7$) algorithm. Events accepted by the trigger simulation are combined to the inclusive jet p_T spectrum in such a way that each p_T bin receives contributions from exactly one fully efficient trigger.

Subsequently, each jet is subjected to a JEC that corrects on average the observed jet energy to the energy of the final state particle jet [25]. Lacking collision data the JEC is currently derived from Monte Carlo truth by matching reconstructed jets with generated particle jets. Due to the fact that the QCD jet p_T spectrum is steeply falling an additional unsmearing step becomes necessary. There are more jets migrating to higher transverse momenta than in the opposite direction because of the finite jet energy resolution. To remove this distortion from the measured spectrum the *Ansatz Method* is used, which has been employed successfully at the Tevatron [24, 26]. The corrected $p_{\mathrm{T,jet}}$ spectra (times K factors) for three regions in absolute rapidity $|y| = \left|\frac{1}{2}\ln\left(\frac{E+p_z}{E-p_z}\right)\right|$ are compared to theory predictions (times non-perturbative corrections) in figure 3 left.

The smeared *Ansatz Function* which has been fitted to the measured spectrum is also used to derive the uncertainties associated with a flat (in $p_{\mathrm{T,jet}}$) 10% jet energy scale uncertainty as well as a 10% variation relative to the nominal value of the JER as estimated in [27]. The result including an assumed initial 10% uncertainty on the luminosity is shown in figure 4 left together with a summary of the associated theory uncertainties on the right. The latter have been evaluated using NLOJET++ [28] and fastNLO [29] for the PDF (CTEQ6.5 [30]) as well as scale uncertainties and the difference between PYTHIA [31] and HERWIG++ [32] for the non-perturbative corrections.

Despite rather large experimental uncertainties initially, some signals of new physics like contact interactions would be observable already at start-up in jet cross sections at transverse momenta beyond Tevatron energies. This is demonstrated in figure 3 right where a contact interaction term corresponding to a compositeness scale of $\Lambda^+ = 3\,\mathrm{TeV}$ is drawn in addition to a pure PYTHIA QCD prediction.

3.2 Dijets

Another possibility to search for new phenomena already at start-up with about $100\,\mathrm{pb}^{-1}$ of integrated luminosity is to look for resonances in the dijet mass spectrum e.g. from the decay of spin-2 Randall-Sundrum gravitons, spin-1 Z' bosons or spin-1/2 excited quarks q^* as presented in [33] for $\sqrt{s} = 14\,\mathrm{TeV}$. Since these resonances exhibit a more isotropic decay angular distribution than dijets from QCD, it is possible to reduce or eliminate the sensitivity to the dominant sources of experimental uncertainty from the JEC respectively the luminosity determination by examining only the ratio of the cross section in two different regions in pseudorapidity. Figure 5 left shows the resulting ratios of $\sigma_{\mathrm{dijet}}(|\eta_j| < 0.7)$ to $\sigma_{\mathrm{dijet}}(0.7 < |\eta_j| < 1.3)$ for three different resonance masses which come out to be significantly larger than for QCD. Figure 5 right illustrates for three different masses of a potential q^* resonance the observable dijet mass spectrum in comparison to QCD including statistical uncertainties as expected for $100\,\mathrm{pb}^{-1}$.

[2)] Forward jets with $3 < |\eta| < 5$ have been investigated in [21] for $\sqrt{s} = 14\,\mathrm{TeV}$.

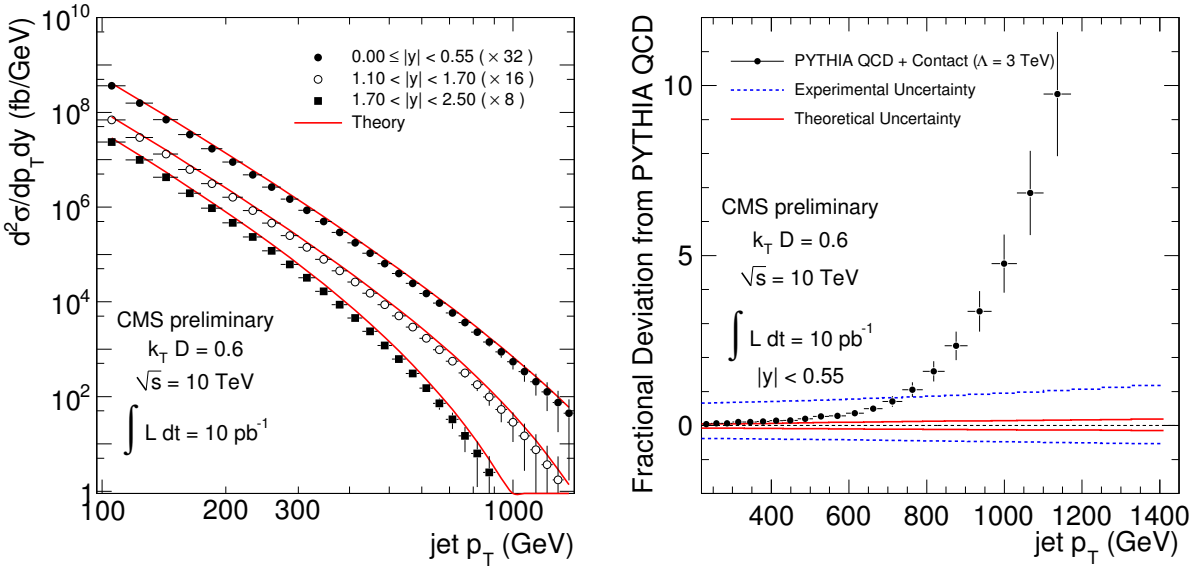

Figure 3: Comparison between the corrected measured spectra and the theory predictions for the k_{T} algorithm (left). For better visibility the spectra have been multiplied by factors of 8, 16 and 32. Fractional difference of a PYTHIA QCD+3 TeV contact interaction term and pure PYTHIA QCD in comparison to the experimental and theoretical uncertainties (right).

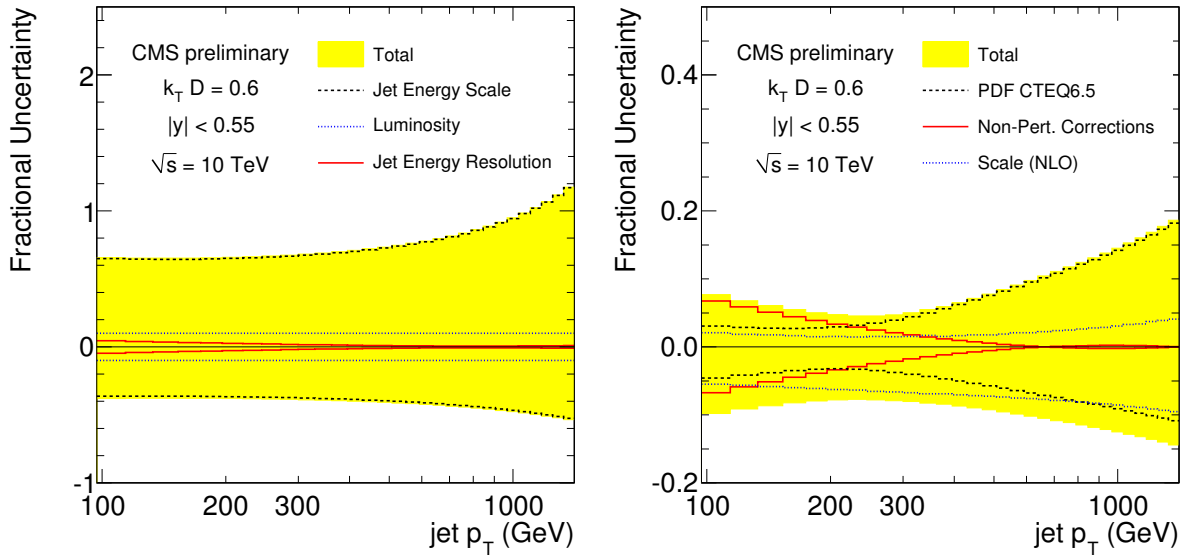

Figure 4: Fractional experimental (left) and theoretical (right) systematic uncertainties at central rapidity for the k_{T} jet algorithm. For better visibility the y-axis ranges have been chosen differently.

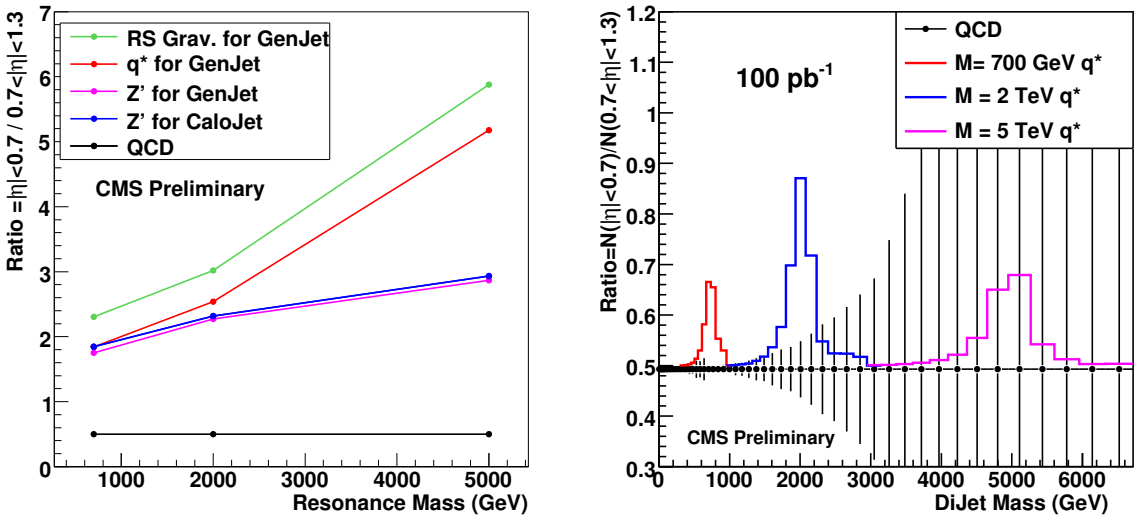

Figure 5: Dijet cross-section ratios in pseudorapidity versus resonance mass for spin-2 Randall-Sundrum gravitons, spin-1 Z' bosons, spin-1/2 excited quarks q^* and QCD (left). Dijet ratio versus resonance mass for three different excited quark masses compared to QCD (right) with statistical uncertainties as expected for $100\,\text{pb}^{-1}$ of integrated luminosity at $\sqrt{s} = 14\,\text{TeV}$.

3.3 Dijet azimuthal Decorrelations

In the study [34] of the normalized dijet cross section $\frac{1}{\sigma_{\text{dijet}}} \cdot \frac{d\sigma_{\text{dijet}}}{d\Delta\varphi_{\text{dijet}}}$ emphasis is put on the angular correlation in azimuth between the two leading jets reconstructed from simulated energy depositions in the calorimeters. Angular quantities in general can be measured more precisely than the energy of jets as here the JEC uncertainty only affects the classification of events into different bins of the leading jet p_{T}. The remaining total systematic uncertainty including effects of the JER and the required unsmearing using different MC generators is estimated to vary approximately linearly from 5% at $\Delta\varphi_{\text{dijet}} = \pi$ to 10% at $\Delta\varphi_{\text{dijet}} = 5\pi/9$. In Figure 6 the corrected $\Delta\varphi_{\text{dijet}}$ distributions from simulated PYTHIA events are compared in several bins of leading jet p_{T} with the predictions of several MC generators and with LO as well as NLO pQCD.

3.4 Event Shapes

Normalized hadronic event shape distributions of e.g. central transverse thrust $\tau_{\perp,\mathcal{C}}$ [35] which have been analyzed in [36] are somewhat similar to the previous observable in the sense that they characterize the geometric momentum flow within an event. Only they usually exploit the complete four-vectors of the measured objects. The sensitivity to the JEC is then reduced by normalizing the quantity derived from the four-vectors to the momentum sum. In general, event shapes, which have also been measured in e^+e^- and ep collisions, do not necessarily require the use of jet algorithms. In this study, however, the shape defining objects have been chosen to be jets reconstructed from simulated energy depositions in the calorimeters with pseudorapidities up to $|\eta| < 1.3$. Figure 7 shows the $\tau_{\perp,\mathcal{C}}$ distribution for k_{T} jets with jet size $D = 0.6$ including statistical and systematic uncertainties from JEC and JER for assumed $10\,\text{pb}^{-1}$ of integrated luminosity at $\sqrt{s} = 14\,\text{TeV}$ together with the MC predictions from PYTHIA and ALPGEN. With higher transverse momenta more events approach thrust values corresponding to a dijet configuration ($\tau_{\perp,\mathcal{C}} \to 0$) as can be seen from a comparison of the distributions for two different minimal transverse energies of the leading jet in figure 7 left and right. Early measurements of event shapes allow to study differences in the modelling of QCD multi-jet production and are a valuable input to MC generator tuning.

3.5 Jet Shapes

As the last topic to be covered in this note jet shapes look into the internal structure of jets. Two observables are suggested in [37] and [38]: The fractional transverse momentum $1 - \psi(R)$ of a jet outside the jet core with a radius of $R = 0.2$ and the second central moment of the jet transverse profile $\langle \delta R_c^2 \rangle$. To explore the largest jet p_{T} range possible, the first quantity has been evaluated for the two leading calorimeter jets from QCD dijet production and is compared in figure 8 with the MC prediction of PYTHIA for quark and gluon jets. The total

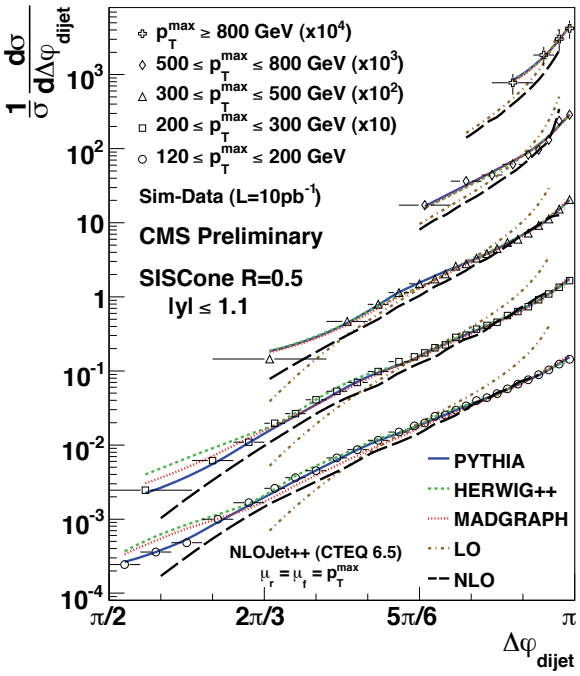

Figure 6: Corrected $\Delta\varphi_{\text{dijet}}$ distributions reconstructed from simulated energy depositions in the calorimeters (black symbols) are presented in several bins of leading jet p_{T} together with the statistical uncertainties as expected for $10\,\text{pb}^{-1}$ of integrated luminosity at $\sqrt{s} = 10\,\text{TeV}$. In addition, the distributions are compared to the particle jet predictions from PYTHIA (full), HERWIG++ (short-dashed), MADGRAPH (dotted), and the predictions from LO (dash-dotted) and NLO pQCD (long-dashed line).

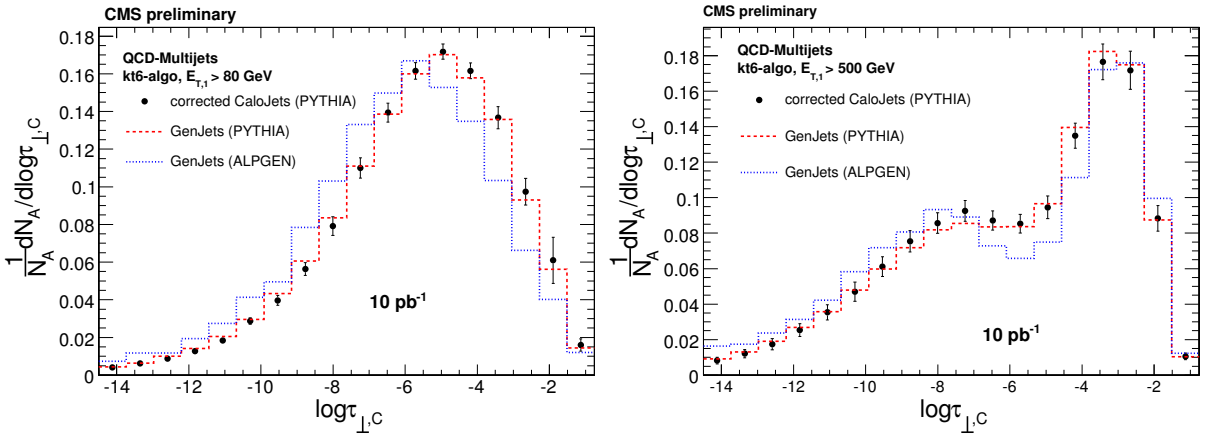

Figure 7: The central transverse thrust distribution ($\tau_{\perp,C}$, in logarithmic scale) reconstructed from simulated energy depositions in the calorimeters (black points) is presented for $E_{\text{T},1}^{\text{cor}} > 80\,\text{GeV}$ (left) and $E_{\text{T},1}^{\text{cor}} > 500\,\text{GeV}$ (right) together with the statistical and dominant systematic uncertainties as expected for $10\,\text{pb}^{-1}$ of integrated luminosity at $\sqrt{s} = 14\,\text{TeV}$. A trigger pre-scale of 100 is assumed in the left plot. In addition, the distributions are compared to the generator predictions of PYTHIA (dashed) and ALPGEN (dotted line).

uncertainty is dominated at low p_{T} by systematic uncertainties due to the JEC, non-linearities of the calorimeter and fragmentation model dependencies estimated using PYTHIA and HERWIG++. At high p_{T} the uncertainty due to lack of statistics with only $10\,\mathrm{pb}^{-1}$ at $\sqrt{s} = 14\,\mathrm{TeV}$ takes over.

To reduce the sensitivity to the JEC and non-linearities in the calorimeters the second central moment $\langle \delta R_c^2 \rangle$ has been calculated for jets where the tracks of charged particles ($p_{\mathrm{T}} > 1\,\mathrm{GeV}$) associated with a jet are used to correct the calorimetric energy determination [39]. The jet substructure then is derived from tracks respectively the charged particles alone. Instead of 10% JEC uncertainty in the former study only $\approx 5\%$ are assumed in the latter. Figure 9 compares the result for $\langle \delta R_c^2 \rangle$ with the MC prediction of HERWIG++ for quark and gluon jets.

Both observables will serve as input for tuning MC generators, in particular with respect to fragmentation models, and may allow an extraction of the quark-gluon jet fraction.

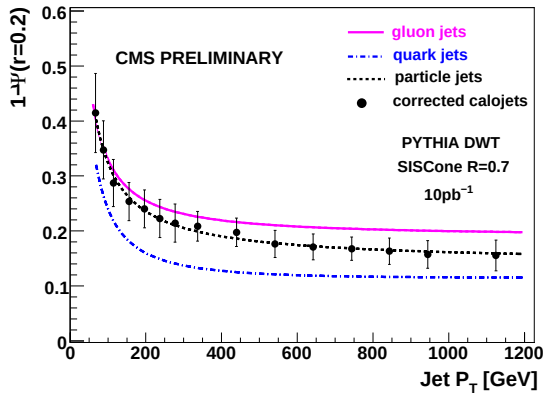

Figure 8: The fractional transverse momentum of a jet outside R=0.2, $1-\psi(0.2)$, is presented versus $p_{\mathrm{T,jet}}$ for jets reconstructed from simulated energy depositions in the calorimeters (black points) in the rapidity region $|y| < 1$ including statistical and systematic uncertainties as expected for $10\,\mathrm{pb}^{-1}$ of integrated luminosity at $\sqrt{s} = 14\,\mathrm{TeV}$. In addition, PYTHIA (tune DWT) predictions are shown for quark initiated (dash-dotted), gluon initiated (solid), and for all particle jets (dashed line).

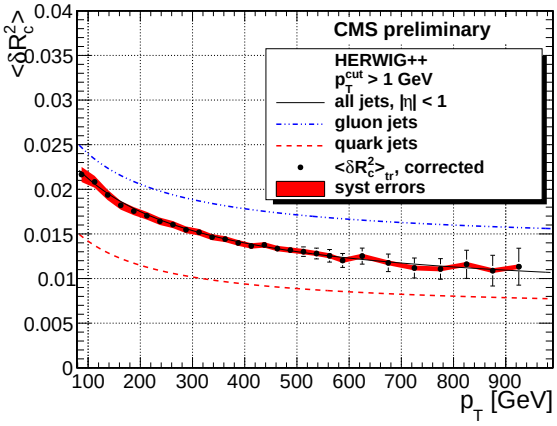

Figure 9: The second central moment $\langle \delta R_c^2 \rangle$ of the jet transverse energy distribution is presented versus $p_{\mathrm{T,jet}}$ for jets reconstructed from tracks (black points) in the pseudorapidity region $|\eta| < 1$ including statistical uncertainties as expected for $10\,\mathrm{pb}^{-1}$ of integrated luminosity at $\sqrt{s} = 10\,\mathrm{TeV}$. The total systematic uncertainty is indicated by the shaded region. In addition, HERWIG++ predictions using charged particles are shown for quark (dashed) and gluon initiated jets (dash-dotted line).

4 Outlook

A number of QCD analyses involving charged particle tracks and jets possible already after a few days of data taking or after accumulating roughly 10 to $100\,\mathrm{pb}^{-1}$ of integrated luminosity have been presented. A rich program of new physics measurements re-establishing the Standard Model and preparing the arena for searches for new phenomena will be possible. CMS is well prepared and first proton-proton collisions at the LHC are eagerly awaited.

5 Acknowledgements

I would like to thank the conference organizers for the kind invitation and for the overwhelming hospitality I had the occasion to encounter. I would also like to thank Kirsti Aspola for her kind organizational help.

References

[1] **CMS** Collaboration, "The CMS experiment at the CERN LHC," *JINST* **0803** (2008) S08004. doi:10.1088/1748-0221/3/08/S08004.

[2] **CMS** Collaboration, "CMS technical design report, volume II: Physics performance," *J. Phys.* **G34** (2007) 995–1579. doi:10.1088/0954-3899/34/6/S01.

[3] P. Gupta, B. C. Choudhary, S. Chatterji, and S. Bhattacharya, "Study of direct photon plus jet production in CMS experiment at $\sqrt{s}$ = 14-TeV," *Eur. Phys. J.* **C53** (2008) 49–58. doi:10.1140/epjc/s10052-007-0460-y.

[4] **UA5** Collaboration, G. J. Alner et al., "Scaling of Pseudorapidity Distributions at c.m. Energies Up to 0.9-TeV," *Z. Phys.* **C33** (1986) 1–6. doi:10.1007/BF01410446.

[5] **CDF** Collaboration, F. Abe et al., "Pseudorapidity distributions of charged particles produced in $\bar{p}p$ interactions at $\sqrt{s} = 630$ GeV and 1800 GeV," *Phys. Rev.* **D41** (1990) 2330. doi:10.1103/PhysRevD.41.2330.

[6] **CMS** Collaboration, "Pseudorapidity distributions of charged hadrons in minimum-bias p-p collisions at $\sqrt{s} = 14\,\mathrm{TeV}$," *CMS Physics Analysis Summary* **CMS-PAS-QCD-08-004** (2008).

[7] **CMS** Collaboration, "Measurement of charged hadron spectra in proton-proton collisions at $\sqrt{s} = 14\,\mathrm{TeV}$," *CMS Physics Analysis Summary* **CMS-PAS-QCD-07-001** (2007).

[8] **CMS** Collaboration, "Study of Charged Hadron Multiplicity in Minimum Bias p+p Collisions at $\sqrt{s} = 900\,\mathrm{GeV}$ and $10\,\mathrm{TeV}$," *CMS Physics Analysis Summary* **CMS-PAS-QCD-09-002** (2009).

[9] **PHOBOS** Collaboration, B. B. Back et al., "Charged particle pseudorapidity density distributions from Au+Au collisions at $\sqrt{s_{NN}}$ = 130-GeV," *Phys. Rev. Lett.* **87** (2001) 102303, arXiv:nucl-ex/0106006. doi:10.1103/PhysRevLett.87.102303.

[10] **PHOBOS** Collaboration, B. B. Back et al., "Charged particle multiplicity near mid-rapidity in central Au + Au collisions at $S^{(1/2)}$ = 56-A/GeV and 130- A/GeV," *Phys. Rev. Lett.* **85** (2000) 3100–3104, arXiv:hep-ex/0007036. doi:10.1103/PhysRevLett.85.3100.

[11] **CMS** Collaboration, "Measurement of the Underlying Event in Jet Topologies using Charged Particle and Momentum Densities," *CMS Physics Analysis Summary* **CMS-PAS-QCD-07-003** (2007).

[12] **CDF** Collaboration, A. A. Affolder et al., "Charged jet evolution and the underlying event in $p\bar{p}$ collisions at 1.8 TeV," *Phys. Rev.* **D65** (2002) 092002.

[13] **CDF** Collaboration, D. E. Acosta et al., "The underlying event in hard interactions at the Tevatron $\bar{p}p$ collider," *Phys. Rev.* **D70** (2004) 072002, arXiv:hep-ex/0404004. doi:10.1103/PhysRevD.70.072002.

[14] D. Acosta, M. Della Negra, L. Fo, A. Herv, and A. Petrilli, eds., "CMS Physics: Technical Design Report, Volume I: Detector Performance and Software", volume LHCC-2006-001 of *Technical Design Report CMS*. CERN, Geneva, 2006.

[15] G. P. Salam and G. Soyez, "A practical Seedless Infrared-Safe Cone jet algorithm," *JHEP* **05** (2007) 086, arXiv:0704.0292.

[16] S. D. Ellis and D. E. Soper, "Successive combination jet algorithm for hadron collisions," *Phys. Rev.* **D48** (1993) 3160–3166, arXiv:hep-ph/9305266.

[17] S. Catani, Y. L. Dokshitzer, and B. R. Webber, "The K-perpendicular clustering algorithm for jets in deep inelastic scattering and hadron collisions," *Phys. Lett.* **B285** (1992) 291–299. doi:10.1016/0370-2693(92)91467-N.

[18] S. Catani, Y. L. Dokshitzer, M. H. Seymour, and B. R. Webber, "Longitudinally invariant K(t) clustering algorithms for hadron hadron collisions," *Nucl. Phys.* **B406** (1993) 187–224. doi:10.1016/0550-3213(93)90166-M.

[19] M. Cacciari and G. P. Salam, "Dispelling the N**3 myth for the k(t) jet-finder," *Phys. Lett.* **B641** (2006) 57–61, arXiv:hep-ph/0512210.

[20] **CMS** Collaboration, "Initial Measurement of the Inclusive Jet Cross Section at $10\,\mathrm{TeV}$ with CMS," *CMS Physics Analysis Summary* **CMS-PAS-QCD-08-001** (2009).

[21] **CMS** Collaboration, "Jet reconstruction in the CMS Forward Hadron (HF) calorimeter in proton-proton collisions at $\sqrt{s} = 14\,\mathrm{TeV}$," *CMS Physics Analysis Summary* **CMS-PAS-FWD-08-001** (2008).

[22] **CDF** Collaboration, T. Aaltonen et al., "Measurement of the Inclusive Jet Cross Section at the Fermilab Tevatron p-pbar Collider Using a Cone-Based Jet Algorithm," *Phys. Rev.* **D78** (2008) 052006, arXiv:0807.2204. doi:10.1103/PhysRevD.78.052006.

[23] **CDF - Run II** Collaboration, A. Abulencia et al., "Measurement of the Inclusive Jet Cross Section using the k_{T} algorithmin$p\bar{p}$ Collisions at$\sqrt{s}$ = 1.96 TeV with the CDF II Detector," *Phys. Rev.* **D75** (2007) 092006, arXiv:hep-ex/0701051. doi:10.1103/PhysRevD.75.092006.

[24] **D0** Collaboration, V. M. Abazov et al., "Measurement of the inclusive jet cross section in $p\bar{p}$ collisions at $\sqrt{s} = 1.96\mathrm{TeV}$," *Phys. Rev. Lett.* **101** (2008) 062001, arXiv:0802.2400. doi:10.1103/PhysRevLett.101.062001.

[25] **CMS** Collaboration, "Plans for Jet Energy Corrections at CMS," *CMS Physics Analysis Summary* **CMS-PAS-JME-07-002** (2008).

[26] **D0** Collaboration, B. Abbott et al., "High-p_T jets in $\bar{p}p$ collisions at $\sqrt{s} = 630$ GeV and 1800 GeV," *Phys. Rev.* **D64** (2001) 032003, arXiv:hep-ex/0012046. doi:10.1103/PhysRevD.64.032003.

[27] **CMS** Collaboration, "Measurement of the Jet Energy Resolutions and Jet Reconstruction Efficiency at CMS," *CMS Physics Analysis Summary* **CMS-PAS-JME-09-007** (2009).

[28] Z. Nagy, "Three-jet cross sections in hadron hadron collisions at next-to-leading order," *Phys. Rev. Lett.* **88** (2002) 122003, arXiv:hep-ph/0110315. doi:10.1103/PhysRevLett.88.122003.

[29] T. Kluge, K. Rabbertz, and M. Wobisch, "Fast pQCD calculations for PDF fits," arXiv:hep-ph/0609285.

[30] W. K. Tung et al., "Heavy quark mass effects in deep inelastic scattering and global QCD analysis," *JHEP* **02** (2007) 053, arXiv:hep-ph/0611254.

[31] T. Sjostrand, S. Mrenna, and P. Skands, "PYTHIA 6.4 physics and manual," *JHEP* **05** (2006) 026, arXiv:hep-ph/0603175.

[32] M. Bahr et al., "Herwig++ Physics and Manual," *Eur. Phys. J.* **C58** (2008) 639–707, arXiv:0803.0883. doi:10.1140/epjc/s10052-008-0798-9.

[33] **CMS** Collaboration, "CMS Search Plans and Sensitivity to New Physics using Dijets," *CMS Physics Analysis Summary* **CMS-PAS-SBM-07-001** (2007).

[34] **CMS** Collaboration, "Dijet Azimuthal Decorrelations in pp Collisions at $\sqrt{s} = 10\,\mathrm{TeV}$," *CMS Physics Analysis Summary* **CMS-PAS-QCD-09-003** (2009).

[35] A. Banfi, G. P. Salam, and G. Zanderighi, "Resummed event shapes at hadron hadron colliders," *JHEP* **08** (2004) 062, arXiv:hep-ph/0407287.

[36] **CMS** Collaboration, "Study of Hadronic Event-Shape Variables," *CMS Physics Analysis Summary* **CMS-PAS-QCD-08-003** (2008).

[37] **CMS** Collaboration, "Transverse Momentum Distribution within Jets in pp Collisions at $14\,\mathrm{TeV}$," *CMS Physics Analysis Summary* **CMS-PAS-QCD-08-005** (2008).

[38] **CMS** Collaboration, "Study of jet transverse structure using the second moment of the jet profile in transverse momentum in pp collisions at $\sqrt{s} = 10\,\mathrm{TeV}$," *CMS Physics Analysis Summary* **CMS-PAS-QCD-08-002** (2009).

[39] **CMS** Collaboration, "Jet Plus Tracks Algorithm for Calorimeter Jet Energy Corrections in CMS," *CMS Physics Analysis Summary* **CMS-PAS-JME-09-002** (2009).